Nanoscale

Paper

Fabrication, Characterization, and High Temperature Surface Enhanced Raman Spectroscopic Performance of SiO_2 Coated Silver Particles

Received 00th January 20xx,
Accepted 00th January 20xx

DOI: 10.1039/x0xx00000x

www.rsc.org/

Ming Liu,[a] Rong Xiang,[*a] Yaerim Lee,[a] Keigo Otsuka,[a] Ya-Lun Ho,[a] Taiki Inoue,[a] Shohei Chiashi,[a] Jean-Jacques Delaunay,[a] Shigeo Maruyama[*a,b]

We present a systematic study on fabrication, characterization and high temperature surface enhanced Raman spectroscopic (SERS) performance of SiO_2 coated silver nanoparticles (Ag@SiO_2) on a flat substrate, aiming to obtain a thermal robust SERS substrate for the monitor of high temperature reactions. We confirm that a 10-15 nm SiO_2 coating provide a structure stability up to 900°C without significantly sacrificing enhancement factor, while the un-coated particle cannot retain SERS effect above 500°C. Finite difference time domain method (FDTD) simulation results supported that SiO_2 coating almost have no influence on the distribution of the electric field but only physically trapped the most enhanced spot inside the coating layer. On this thermally robust substrate, we confirmed the SERS of horizontally aligned single walled carbon nanotubes are stable at elevated temperatures, and demonstrate an in situ Raman monitoring on the atmosphere annealing process of nanodiamonds, in which the interconverting process of C-C bonds is un-ambitiously observed. We claim this is a first experimental proof that high temperature SERS effect can be preserved and applied in a chemical reaction at temperature above 500°C. This versatile substrate also enables novel opportunities for observing growth, etching, and structure transformation of many 0D and 2D nano-materials.

Introduction

Surface enhanced Raman scattering (SERS), discovered by Jeanmaire and Van Duyne on roughened Ag electrodes in 1977,[1] has attracted exponentially increasing attention because of its ability to provide non-destructive and ultra-sensitive characterization of a wide variety of analytes at extremely low concentrations.[2] It has been found to be an important spectroscopy approach in identifying chemical species and obtaining structural information in many fields like biosensing,[3-5] chemical detecting,[6, 7] and electrochemistry.[8] Jeanmaire and Van Duyne, and Albrecht and Creighton have proved that an enhancement in the Raman signal was due to a localized electromagnetic field around the metallic nanostructures (e.g. Au, Ag and Cu).[1, 9, 10] Typically, different metal are SERS effective at different wavelengths, and silver nanostructures are considered as the most common SERS active species due to their unique plasmonic properties, which lead to a higher enhanced effect of the Raman scattering compared to other materials in visible range.[10]

Due to the high sensitivity in detecting structure change, one possible application field for SERS is *in situ* monitoring a catalytic reaction. However, many catalytic reaction need a high temperature environment while almost all previous research on SERS are measured at room temperature only. There are still a number of limitations associated with current SERS field at elevated temperatures. For example, nanostructures rapidly lose their enhancement capabilities in a short period of time under high-temperature conditions due to surface oxidation (for Ag) and aggregation process.[11-14] Moreover, high temperature SERS theory has not been intensively explored, although there are several theoretical studies predicting that SERS enhancement ratio decreases at elevated temperature at scattering frequencies close to the surface plasmon resonance.[15, 16] However, if the excitation wavelength is above the surface plasmon resonance, SERS effect is relatively insensitive to temperature.[15] Therefore, a prerequisite for successful applications of nanostructures in monitoring catalyst reaction and SERS-based sensors at elevated temperature is to maintain the morphology of structure robust at high temperatures and investigate the high temperature SERS mechanism.

One studying system of focused research interest is catalytic synthesis, or transformation of nano-carbon materials. Though SERS is extremely sensitive in detecting molecules of a biomedical or national security interest,[17-20] it has received only a limited attention in the study of catalysis,[21-23] especially real time monitoring catalyst reaction like the growth process of nano-carbon materials, e.g. single-walled carbon nanotubes (SWNTs) and nano-diamond. There are several reports on *in situ* monitoring Raman scattering of SWNTs

[a] *Department of Mechanical Engineering, The University of Tokyo, Tokyo 113-8656, Japan.*
E-mail: maruyama@photon.t.u-tokyo.ac.jp; xiangrong@photon.t.u-tokyo.ac.jp
[b] *Energy NanoEngineering Laboratory, National Institute of Advanced Industrial Science and Technology (AIST), Tsukuba 305-8564, Japan*

Electronic Supplementary Information (ESI) available: [IV curve of SERS substrate, comparison of SEM images and SERS effect between original Ag nanoparticles and Ag nanoparticles after annealing at 900°C, temperature-dependent *in situ* Raman spectra of nanodiamonds during thermally annealed process on silicon wafer, schematic illustration of 3D FDTD simulation mode]. See DOI: 10.1039/x0xx00000x

during growth process. For example, Chiashi et al. revealed that the G-band intensity increased nearly linearly with time after the initial rapid increase during the growth process;[24] Navas et al. investigated the evolutions of nanotube diameter distribution during the growth by *in situ* Raman scattering.[25] In general, however, the G-band Raman signal obtained at a high temperature is always too weak and broad to explicitly recognize the structure-relating fingerprints.[26-28] In our previous work,[29] we proposed to use silver nanoparticle to enhance the Raman scattering of SWNTs during growth, and confirmed that SERS effect of silver nanoparticles was stable and insensitive to elevated temperature at the same morphology. The drawbacks of this previous strategy is the morphology degradation at high temperature lead to a significant decrease in the SERS signal, i.e. the thermal stability of metal particles became the limitation for further using SERS in monitoring a high temperature reaction.

In this work, we are devoted to improve the high temperature stability of SERS substrate by sputtering thermally robust silicon dioxide (SiO_2) thin layer on Ag nanoparticles to form a structure consisting of Ag core capped by SiO_2 shell. We perform a systematic investigation on the fabrication, structure optimization, and SERS characterize of Ag@SiO_2 at room and high temperatures. A sub 15 nm SiO_2 coating is proven to be able to provide a structure stability up to 900°C without significantly sacrificing enhancement factor. A clear and thermal stable SERS enhancement was observed during the heating process of horizontally aligned (HA-) SWNTs. Furthermore, *in situ* monitoring thermal annealing of nanodiamonds with few orders of magnitudes enhancement is demonstrated on this SERS substrates. Finally, finite difference time domain (FTDT) simulation provided a verification about the SERS mechanism of this structure.

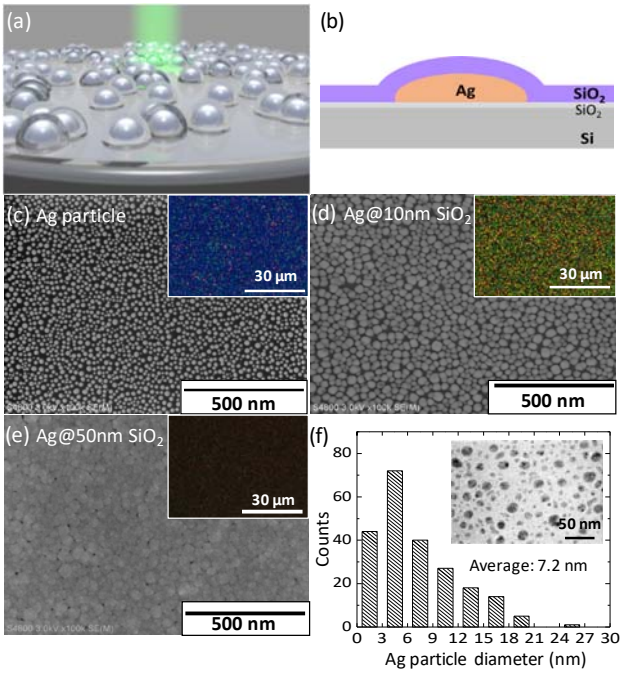

Fig.1 (a). Schematic illustration of Ag nanoparticle coating by SiO_2 on substrate under the laser excitation; (b) Schematic illustration of sectional view of Ag nanoparticle coating by SiO_2 on substrate; (c-e) Representative SEM images of Ag particle, Ag coating by 10nm SiO_2, Ag coating by 50 nm SiO_2, and corresponding dark field images (inset); (f) Histogram of diameter distribution of Ag nanoparticle inside SiO_2 coating layer and a representative TEM image.

Results and Discussions

Figure 1a shows a schematic of our strategy using SiO_2 coating to prevent the migration and aggregation of silver nanoparticles at high temperatures. The choice of SiO_2 is not only because of its high melting point that can enhance thermal stability of the nanoparticles, but also its chemical inertness and capability of supporting the growth many nano-materials including SWNTs. Representative SEM images and corresponding dark field images (inset) of the pure Ag, 10 nm SiO_2 coated Ag (Ag@10nm SiO_2), and 50 nm SiO_2 coated Ag (Ag@50nm SiO_2) are shown in Fig 1c, d, e, respectively. It is clearly seen in SEM images that the morphology of each type of SERS substrate is uniform and silver nanoparticles are isolated on substrate. I-V characterizations (Fig. S1) confirm that the three SERS substrates are insulators, suggesting that particles are well isolated on the substrate. The dark field images reveal strong scattering by the structure interpreted as SERS hot spots. The synthesis of SWNTs was performed on Ag@10nm SiO_2 to prove the capability of this sputtering SiO_2 layer to support the growth of nano-materials. The representative SEM image and Raman spectra of SWNTs synthesized on SERS substrate are shown in Fig. S5.

To obtain the detailed morphology and dimension of the SiO_2 coated particles, we perform TEM characterization using a Si/SiO_2 TEM grid. The fabrication procedure of SiO_2 coated nanoparticles on the grid is the same as on normal silicon wafer, which guarantees that particles on TEM grid possess the same surface morphology and particle size. The typical TEM image of the particle (inset) and histogram of size distribution are shown in Fig. 1e, which suggests the average diameter of inside silver particle is 7.2 nm and the most distributing size is from 3 to 6 nm. This histogram of size distribution was obtained by counting the diameter of particles from one batch of representative sample, however there is an approx. 50% variation of particle size among batches in our experiment for example the average inner Ag particle size in Fig. 4e is slightly different from the result in Fig. 1f.

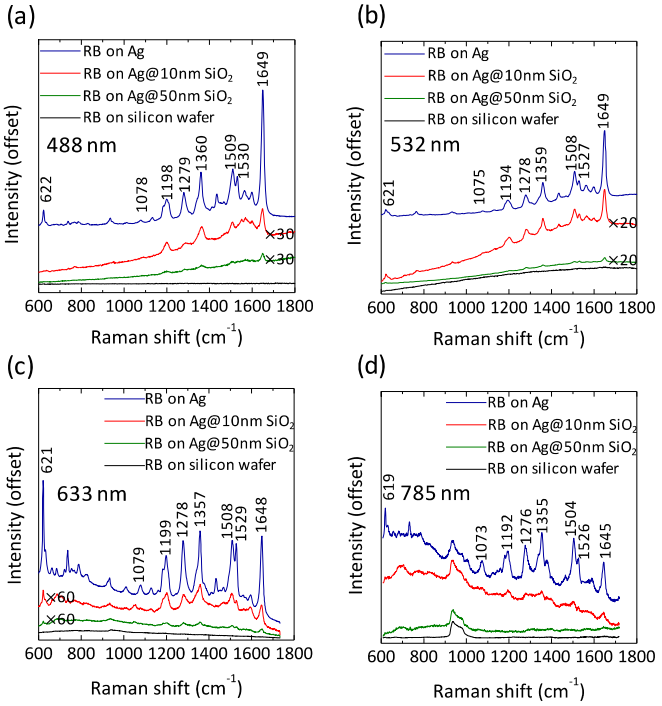

Fig. 2 Raman spectra of Rhodamine B on silicon wafer, Ag nanoparticle, Ag@10nm SiO_2 and Ag@50nm SiO_2 substrates under (a) excitation laser 488 nm; (b) excitation laser 532 nm; (c) excitation laser 633 nm; (d) excitation laser 785 nm.

After the characterization of SERS substrates, Rhodamine B was utilized to confirm the SERS enhancement effect of these substrates. A systematic comparison of SERS effect before and after coating SiO_2 is presented in Fig.2, by detecting standard Rhodamine B ethanol solution with the concentration of 5.3×10^{-4} M. The four wavelengths 488 nm, 532 nm, 633 nm, and 785 nm were used to excite the Raman scattering of rhodamine B on four types of substrate including silicon wafer, pure Ag particles, Ag@10nm SiO_2 and Ag@50nm SiO_2. There is almost no obvious Raman peak of Rhodamine B on silicon wafer (black lines in four graphs), compared with significantly enhanced Raman signal on the other three substrates. Moreover, under the excitation of 785nm, SERS substrates did not show proper enhancement effect, whereas 488nm, 532nm and 633 nm excitations performed stronger enhancement which perfectly match the requirement of the high temperature Raman observation (as high temperature reactions usually come with radiation in red and infrared range). Also according to the Leung's theory, generally the SERS effect of shorter excitation wavelengths is insensitive to temperature while the excitation wavelengths are above the surface plasmon resonance.[15]

For all excitations, the pure Ag shows the strongest enhancement for Rhodamine B, and the six typical Raman peaks of Rhodamine B are indexed on the Raman spectra in Fig. 2. As expected, the enhancement factor decreased with SiO_2 thickness, and when the thickness of SiO_2 layer reaches 50 nm, the enhancement effect almost disappears because of the drastic decrease in the density of scattering spots as showed in Fig. 1e (inset). However, it is encouraging that Ag@10nm SiO_2 (and also Ag@15nm SiO_2, not shown) substrate still exhibits same order of magnitude for the enhancement at room temperature, which is efficient enough to detect many organic pollutants at low concentration. This result suggest that a 10 or 15 nm coating is only reducing the enhancement factor by a few folds. Comparing to orders of magnitude enhancement over the non-SERS condition, this a few folds decrease is nearly negligible. After confirming the SERS effect of these substrates, Ag@10nm SiO_2 substrate was chosen to perform the following high-temperature experiment.

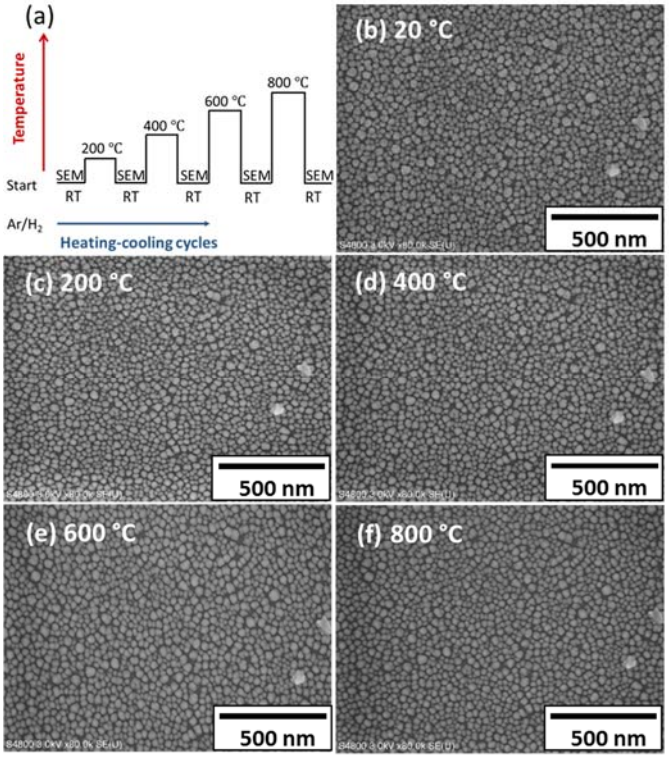

Fig.3 (a) An experimental scheme recording the morphology change with elevated temperature; (b-f) representative SEM images of "Ag@10nm SiO_2" structure after each annealing circle.

Figure 3a shows the heating pattern used for in this study and SEM characterization is performed at the same position at room temperature after different temperature annealing. Briefly the substrates are heated at 200, 400, 600, 800°C to investigate the thermal stability of Ag@10nm SiO_2 substrate. In our previous work, pure Ag film evolved from a continuous film to separate island-like structure during the heating circle starting from room temperature to 800°C. In this work, however, SiO_2 coated Ag nanoparticles successfully retain their spherical shape and size up to 800°C (Fig. 3b-f), which confirms that 10-15 nm SiO_2 layer effectively improves the thermal robustness of Ag nanoparticle. Moreover, the morphology of Ag nanoparticles before and after annealing at 900°C were also characterized by SEM, the typical images are shown in Fig. S2a-b. The Ag nanoparticles were partially evaporated or aggregated during the temperature increase cycles and turned into a totally different morphology when observed after cooling to room temperature. Raman spectra of Rhodamine B before and after the heating process on Ag@10nm SiO_2 and pure Ag nanoparticle substrates (Fig. S3c-d) showed that Ag@10nm SiO_2 substrate maintained stable SERS enhancement after high-temperature treatment.

More precise and quantitative analysis of the difference between Ag@10nm SiO_2 before and after elevating temperature (800°C) is obtained using TEM and the representative images are presented in Fig.4c-d. Fig. 4d shows the typical morphology of Ag@10nm SiO_2

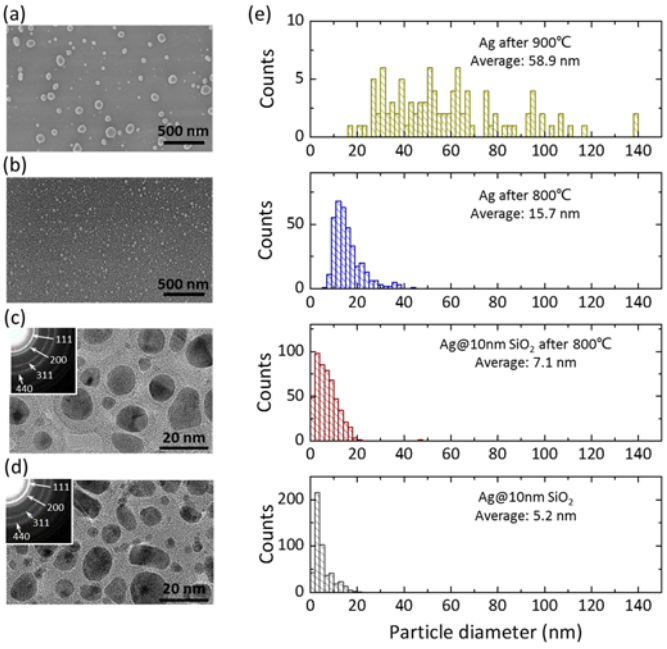

Fig. 4. SEM image of "Ag nanoparticle" structure after annealing at (a)900 °C and (b) 800 °C (particle size is too big for TEM characterizing); (c) Representative TEM image of premier "Ag@10nm SiO_2" structure after annealing at 800 °C and corresponding selected area electron diffraction pattern; (d) Representative TEM image of premier "Ag@10nm SiO_2" structure and corresponding selected area electron diffraction pattern; (e) Histogram of diameter distribution of Ag part in "Ag@10nm SiO_2" structure before and after annealing process and pure Ag particle after annealing at 800 °C and 900 °C.

nanoparticles and Fig. 4c is the TEM image of Ag@10nm SiO_2 nanoparticles after heating to 800°C. In Fig. 4c and d, no clear difference in the morphology of Ag core part is observed between the two samples. In these two observations, we successfully identified the contrast of core shell layer SiO_2 even though the background SiO_2 from TEM grid is pretty strong. Furthermore, one uniqueness of this in-plane TEM is the capability of providing comprehensive structural information in a large area. Hence, the selected area electron diffraction (SAED) patterns of these two samples (Fig. 4c and d (inset)) are taken with the selected area aperture diameter of several micrometers, and contain the average in formation of more than 10,000 particles. From SAED patterns, it is clearly revealed that the crystal structure of Ag maintained after annealing at 800°C.

Figure 4a and 4b show the SEM images of pure Ag nanoparticle after 900°C and 800°C with a protective Ar/H_2(3%) atmosphere. The size of Ag nanoparticles after annealing is too large to be observed using TEM. For annealing after 800°C, the morphology of substrate significantly changed and many large nanoparticles appeared after high temperature treatment. For the 900°C treatment, the morphology of the substrate is totally changed and the particles are larger than the original particles. From the comparison of Fig 4a and 4b, annealing at 900°C has more notable influence on the morphology of Ag nanoparticles because the mobility of surface atom at 900°C is higher than 800°C. The size distribution of Ag core in Ag@10nm SiO_2 nanoparticles is mainly concentrated below 20 nm, as shown in Fig. 4e, and the average diameter of Ag core is 5.2 nm. Similarly, the diameter of Ag core in Ag@10nm SiO_2 nanoparticles after elevating to 800°C is mostly below 20 nm, and the average size is 7.1 nm which is only slightly different from original particles. In contrast, without the protection of SiO_2, the size of the Ag nanoparticles is widely distributed after high temperature treatment and the average size increases to 15.7 nm (800°C) and 58.9 nm (900°C). The TEM characterization indicates that the thermally stable SiO_2 layer coated nanoparticles show a potential to serve as effective operando SERS substrates at high temperature.

After confirming the SERS enhancement Ag@SiO_2 structure at room temperature and its thermal stability at high temperature, we present a preliminary exploration on the application of this high temperature SERS substrates to investigate high-temperature SERS spectra of SWNTs. A horizontally aligned SWNT film synthesised by ACCVD method is transferred on to a Ag@10nm SiO_2 substrate with the assisting of PMMA. Fig. 5a shows comparisons of SERS (red) and non-SERS (blue) spectra of SWNTs taken from 30°C up to 800°C under 488 nm wavelength excitation. A protective Ar/H_2 atmosphere is introduced in the reaction chamber during the entire measurement to prevent oxidation of SWNTs. In Fig. 6a, two representative peaks of SWNTs (G and D band) are clearly enhanced on SiO_2 coated Ag substrate (red curves). Though the overall intensity decrease at elevated temperatures, the enhancement successfully retained up to 800°C.

The G band position of SWNTs on SERS (red) and non-SERS (blue) area vs. temperature is plotted in Fig. 5b. There are at least two main changes to the Raman spectra in comparisons. First, G band position of SERS and non-SERS spectra shares the same trend that down shift lower wavenumbers, which has been well verified in previous studies and can be illustrated by the tube structure expansion and C-C bond softening at high temperature.[30-32] Secondly, there are small shifts (~3 cm^{-1}) in G band to lower wavenumber on Ag@10nm SiO_2 substrate compared to non-SERS part, which is one typical feature of SERS effect. Moreover, the enhancement factor vs. temperature is showed in Fig. 5c, in which clear enhancements can be observed at all temperatures. Besides, there is no obvious drop of enhancement factor with temperature although the enhancement factor of around 3 is quite

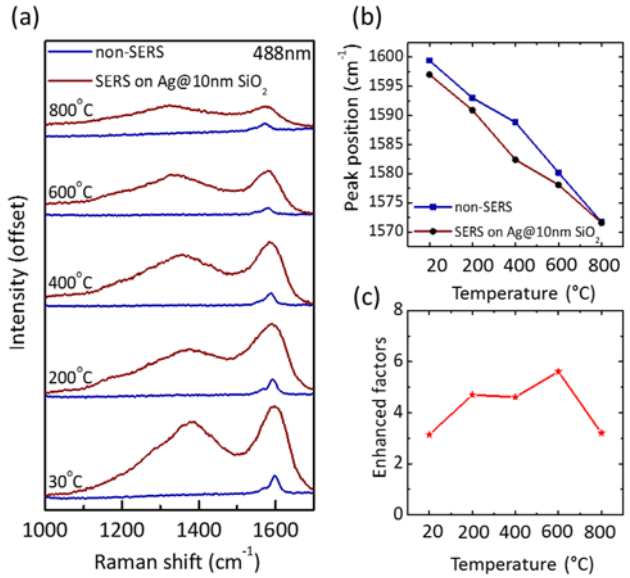

Fig. 5 (a) Non-SERS spectra of HA-SWNT on SiO_2 substrate and SERS spectra of the same HA-SWNT on "Ag@10nm SiO_2" substrate at different temperatures (excitation laser 488 nm); (b) G-band position of HA-SWNT on non-SERS and SERS substrate at different temperatures; (c) SERS enhanced factors of HA-SWNT at different temperatures.

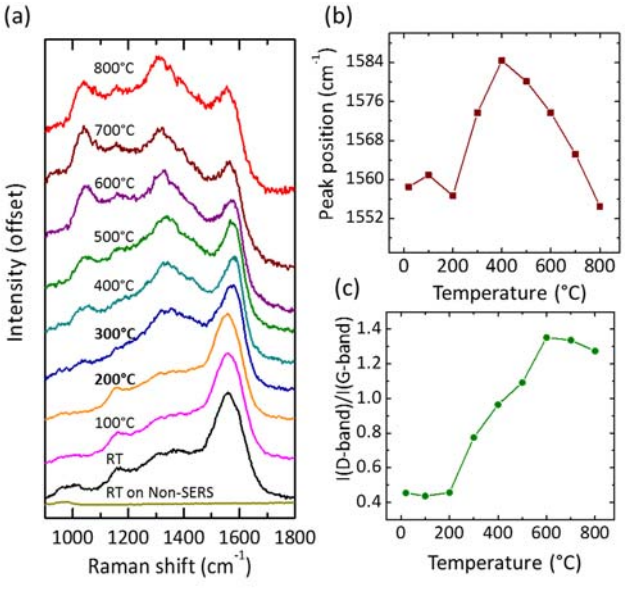

Fig. 6 (a) Temperature-dependent *In situ* Raman spectra of nanodiamonds during thermally annealed process on Ag@10nm SiO_2 substrate; (b) The G-band positions from analysis of the temperature-dependent *in situ* Raman spectra as a functions of temperature; (c) The ratio of the intensities of D-band to G-band from the analysis of the temperature-dependent *in situ* Raman spectra as a functions of temperature.

small. Here we claim this enhancement factor for SWNTs is the entire effect for all SWNTs due to their 1D geometric characteristics, the intrinsic enhancement at local hot spot should be much higher than this value.

Much more notable enhancements were observed when nano-diamond, a 0D material, is tested on this SiO_2 coated Ag substrate. In this part, nanodiamonds in ethanol solution was dropped on the Ag@10nm SiO_2 SERS substrate and performed high temperature annealing process in Ar/H_2 (3%) atmosphere. The representative *in situ* Raman spectra of nanodiamonds at different elevated temperatures on SERS substrate are shown in the Fig. 6a, in comparison the Raman spectra in the same condition on the normal silicon wafer are shown in Fig. S3a. Before enhancement, there are almost no obvious structure-related fingerprint peak in the Raman spectra of nanodiamonds on normal silicon wafer (non-SERS spectrum in Fig. 6a). However, there are a SERS enhancement of nanodiamonds on Ag@10nm SiO_2 substrate from room temperature to harsh elevated temperature until 800°C.

Generally, it is assumed that there are mixtures of carbon sp^2 and sp^3 bonds in nanodiamonds and thermal treatment would change the structure of amorphous carbon to a graphitic structure. The G band (1560 cm^{-1}) positions and the intensity ratio of D band (1350 cm^{-1}) to G band (I_D/ I_G) from analysis of the temperature-dependent *in situ* Raman spectra of the thermally annealed nanodiamonds at different temperatures are shown in Fig. 6a and b. During the annealing process, nanodiamonds graphitized gradually from 200°C, which is revealed by the positions of G-bands shift slightly to a higher wave number and I_D/ I_G ratio starts to increase at the same temperature. These results indicate that the interconverting of sp^3 to sp^2 in nanodiamonds began at 200°C and resulted in a stable graphite-like phase at 600 °C. This Ag@10nm SiO_2 substrate provides a possibility to precisely observe the annealing process of nanodiamonds and other chemical reaction at elevated temperatures.

Finally, to shed some lights to the underlying enhancement mechanism from a theoretical aspect and better understanding the influence of the coating SiO_2 on the distribution of electric field, we perform the finite difference time domain method (FDTD)[33, 34] to simulate the intensity of the relative electric field. FDTD method provides a convenient, systematic and general approach for calculating the optical response of plasmonic nanostructures of arbitrary symmetry and geometry to an incident light wave, which transfers the differential equations to difference equations. We adopt a 30 nm Ag sphere placing on the SiO_2 flat substrate as a basic model (Fig. S4a). The plane wave is normally incident on the substrate with p-polarization (inset of Fig. S4a). Two Ag spheres with a gap size of 10 nm, an Ag sphere with 5 nm SiO_2 layer capping, two 5 nm SiO_2 coating Ag spheres, and a random distribution of Ag spheres with and without the 5-nm SiO_2 coating Ag spheres are simulated in this work. Fig. 7a shows the FDTD simulated electric-field distribution of single Ag sphere and Fig. 7b gives the electric-field distribution in the gap between the two Ag nanospheres. From Fig. 7a and b, it is concluded that the strongest electric field enhancement origins from the gap between nanospheres and the "hot spot" in the gap region is highly localized on the surface of each nanospheres. In the random distribution of Ag nanospheres (Fig. 7c), the smaller gaps generate stronger electric field. Fig. 7d, e and f show the similar simulated results for the 5-nm SiO_2 coated nanospheres. The overall distribution of the electric field is not affected by the SiO_2 coating, however the strongest "hot spots" are physically inaccessible because they are excited at the interface between Ag and SiO_2. This may explain the decrease in the SERS signal when compared to the original bare Ag nanospheres. Also SiO_2 coating reduces the inter-distance between all particles, so that some gaps will be closed and lose their activity as hot spots. In average, a smaller number of hot spots may be available after the SiO_2 coating and so the SERS signal should decrease. Nonetheless, the remaining electric field out of the SiO_2 coating nanospheres could still perform noticeable enhancement in the Raman scattering in this work and we demonstrate this structure can enhance the Raman signal stablely at high temperatures.

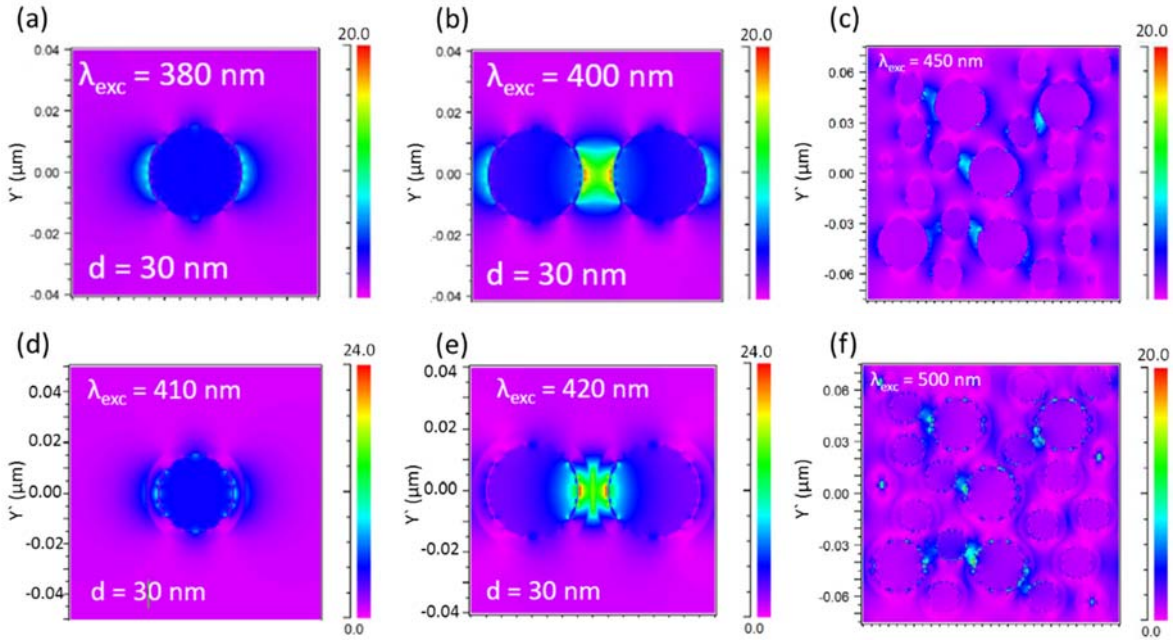

Fig. 7 Simulation results of electric field distribution by FDTD method of (a) single pure Ag nanoparticle; (b) double pure Ag nanoparticles; (c) random distribution of pure Ag particles with different sizes; "Ag@5nm SiO_2" structure (d) single particle; (e) double particles; (f) random distribution of particles with different sizes.

Conclusions

In conclusion, we presented a systematic study on the fabrication, characterization, and SERS effect of SiO_2 coated Ag nanoparticels, aiming to design a thermally stable and versatile substrate for monitoring high temperature catalytic reactions. A SiO_2 coating of 10-15 nm is found to be able to significantly enhance the thermal stability of Ag particle without much sacrificing its SERS effect. TEM and SEM characterizion after testing the structure at elevated temperatures show that the Ag coated by SiO_2 particles were verified to maintain stable and retain the same size and morphology at temperatures up to 900°C. The monitoring of annealing process of nano-diamonds revealed the interconverting of C-C bonds and also explored the possibility of using this substrate to observe other chemical reactions. At last, the FDTD simulation proved that the coating SiO_2 layer did not change the distribution of electric field but only physically trapped the most enhanced spot. We claim this work is a first experimental proof that high temperature SERS effect can be preserved and applied in a chemical reaction at temperature above 500°C, and emphasize that this substrate can be an efficient and versatile SERS substrate to monitor processes such as etching, annealing and growth processes for various material systems (particularly 0D and 2D nanomaterials), possibly including semi-conducting nano-particles, graphene, MoS_2 and/or other 2D materials.

Experimental Methods

Fabrication of SERS Substrates

A thin film of silver (nominal thickness 5 nm) was deposited on an n-type Si substrate with a 100 nm-thick SiO_2 layer (SUMCO technology co., Itd.) by thermal evaporation technique at a background vacuum level of 10^{-5} Pa. After silver deposition, the substrate was annealed at 600°C for 5 min with the protection of Ar diluted H_2 (3%) to form Ag nanoparticles. Finally, different thickness of SiO_2 layers were deposited on the Ag nanoparticles by sputtering. The morphology and structure of Ag nanoparticles and Ag wrapped by SiO_2 layers were characterized by optical microscopy (dark field mode), scanning electron microscopy (SEM; HITACHI-S4800) and transmission electron microscopy (TEM; JEOL 2010F).

Raman Spectroscopy

The SERS spectra were obtained with a Renishaw InVia micro Raman system equipped with a ×20 objective lens. Four different laser lines (488 nm, 532 nm, 633 nm, and 785 nm) were used as the excitation light sources. An ethanol solution containing a 5.3×10^{-4} M rhodamine B ($C_{28}HClN_2O_3$, Wako, CI 45179) was applied to the SERS substrate to verify the enhancement at room temperature. Nanodiamonds were sonicated in the ethanol solution for 30 min and then drop-casted on to the substrate to perform high temperature SERS. Horizontally aligned SWNTs were synthesised using the alcohol catalytic chemical vapour deposition method [35, 36] on r-cut crystal quartz substrates, and then transferred onto the SERS substrates via poly (methyl methacrylate) (PMMA) thin films.[37]

Simulation Model

The 3D finite-difference time-domain technique is used to compute the distribution of the electromagnetic fields of five models and explore the SERS mechanism of the core shell particles. Particularly, the effect of the gap between particles is investigated by reporting the field distribution for dimer arrangement with and without the SiO_2 protective coating. The reported distributions are given for the wavelengths corresponding to the maximum of the electric field component aligned with the dimer symmetry axis.

Acknowledgements

Part of this work is financially supported by JSPS KAKENHI Grant Numbers JP25107002, JP15H05760, JP15K17984, and IRENA Project by JST-EC DG RTD, Strategic International Collaborative Research Program, SICORP. Part of this work is based on results obtained from a project commissioned by the New Energy and Industrial Technology Development Organization (NEDO) and by the "Nanotechnology Platform" (project No. 12024046) of the Ministry of Education, Culture, Sports, Science and Technology (MEXT), Japan.

Notes and references

1. D. L. Jeanmaire and R. P. Van Duyne, *Journal of Electroanalytical Chemistry and Interfacial Electrochemistry*, 1977, **84**, 1-20.
2. J. P. Camden, J. A. Dieringer, J. Zhao and R. P. Van Duyne, *Accounts of chemical research*, 2008, **41**, 1653-1661.
3. A. El-Ansary and L. M. Faddah, *Nanotechnology, science and applications*, 2010, **3**, 65-76.
4. S. D. Hudson and G. Chumanov, *Analytical and bioanalytical chemistry*, 2009, **394**, 679-686.
5. R. A. Tripp, R. A. Dluhy and Y. Zhao, *Nano Today*, 2008, **3**, 31-37.
6. D. A. Stuart, K. B. Biggs and R. P. Van Duyne, *Analyst*, 2006, **131**, 568-572.
7. J. M. Sylvia, J. A. Janni, J. Klein and K. M. Spencer, *Analytical chemistry*, 2000, **72**, 5834-5840.
8. W. F. Paxton, S. L. Kleinman, A. N. Basuray, J. F. Stoddart and R. P. Van Duyne, *The journal of physical chemistry letters*, 2011, **2**, 1145-1149.
9. M. G. Albrecht and J. A. Creighton, *Journal of the American Chemical Society*, 1977, **99**, 5215-5217.
10. M. Kerker, *Accounts of Chemical Research*, 1984, **17**, 271-277.
11. H. Alarifi, A. Hu, M. Yavuz and Y. N. Zhou, *Journal of Electronic Materials*, 2011, **40**, 1394-1402.
12. K. Nanda, A. Maisels, F. Kruis, H. Fissan and S. Stappert, *Physical review letters*, 2003, **91**, 106102.
13. Q. Jiang, S. Zhang and J. Li, *Solid State Communications*, 2004, **130**, 581-584.
14. Z. Z. Fang and H. Wang, *International Materials Reviews*, 2008, **53**, 326-352.
15. P. Leung, M. Hider and E. J. Sánchez, *Physical Review B*, 1996, **53**, 12659.
16. C. Chen, H.-P. Chiang, P. Leung and D. Tsai, *Solid State Communications*, 2008, **148**, 413-416.
17. E. A. Vitol, Z. Orynbayeva, M. J. Bouchard, J. Azizkhan-Clifford, G. Friedman and Y. Gogotsi, *Acs Nano*, 2009, **3**, 3529-3536.
18. T. Vo-Dinh, H. N. Wang and J. Scaffidi, *Journal of biophotonics*, 2010, **3**, 89-102.
19. X. Zhang, J. Zhao, A. V. Whitney, J. W. Elam and R. P. Van Duyne, *Journal of the American Chemical Society*, 2006, **128**, 10304-10309.
20. R. S. Golightly, W. E. Doering and M. J. Natan, *Journal*, 2009.

21. K. N. Heck, B. G. Janesko, G. E. Scuseria, N. J. Halas and M. S. Wong, *Journal of the American Chemical Society*, 2008, **130**, 16592-16600.
22. C. Fokas and V. Deckert, *Applied spectroscopy*, 2002, **56**, 192-199.
23. G. L. Beltramo, T. E. Shubina and M. Koper, *ChemPhysChem*, 2005, **6**, 2597-2606.
24. S. Chiashi, Y. Murakami, Y. Miyauchi and S. Maruyama, *Chemical Physics Letters*, 2004, **386**, 89-94.
25. H. Navas, M. Picher, A. Andrieux-Ledier, F. d. r. Fossard, T. Michel, A. Kozawa, T. Maruyama, E. Anglaret, A. Loiseau and V. Jourdain, *ACS nano*, 2017, **11**, 3081-3088.
26. A. Jorio, C. Fantini, M. Dantas, M. Pimenta, A. Souza Filho, G. G. Samsonidze, V. Brar, G. Dresselhaus, M. Dresselhaus and A. Swan, *Physical Review B*, 2002, **66**, 115411.
27. A. Li-Pook-Than, J. Lefebvre and P. Finnie, *The Journal of Physical Chemistry C*, 2010, **114**, 11018-11025.
28. A. Jorio, M. Pimenta, A. Souza Filho, R. Saito, G. Dresselhaus and M. Dresselhaus, *New Journal of Physics*, 2003, **5**, 139.
29. M. Liu, R. Xiang, W. Cao, H. Zeng, Y. Su, X. Gui, T. Wu, S. Maruyama and Z. Tang, *Carbon*, 2014, **80**, 311-317.
30. A. Jorio, C. Fantini, M. S. S. Dantas, M. A. Pimenta, A. G. Souza Filho, G. G. Samsonidze, V. W. Brar, G. Dresselhaus, M. S. Dresselhaus, A. K. Swan, M. S. Ünlü, B. B. Goldberg and R. Saito, *Physical Review B*, 2002, **66**, 115411.
31. Y. Zhang, L. Xie, J. Zhang, Z. Wu and Z. Liu, *The Journal of Physical Chemistry C*, 2007, **111**, 14031-14034.
32. H. Li, K. Yue, Z. Lian, Y. Zhan, L. Zhou, S. Zhang, Z. Shi, Z. Gu, B. Liu and R. Yang, *Applied Physics Letters*, 2000, **76**, 2053-2055.
33. A. Taflove and S. C. Hagness, *Artech House Boston, London*, 2000.
34. F. Solutions, *Inc., Canada*, 2003.
35. T. Inoue, D. Hasegawa, S. Badar, S. Aikawa, S. Chiashi and S. Maruyama, *The Journal of Physical Chemistry C*, 2013, **117**, 11804-11810.
36. S. Maruyama, R. Kojima, Y. Miyauchi, S. Chiashi and M. Kohno, *Chemical physics letters*, 2002, **360**, 229-234.
37. L. Jiao, B. Fan, X. Xian, Z. Wu, J. Zhang and Z. Liu, *Journal of the American Chemical Society*, 2008, **130**, 12612-12613.